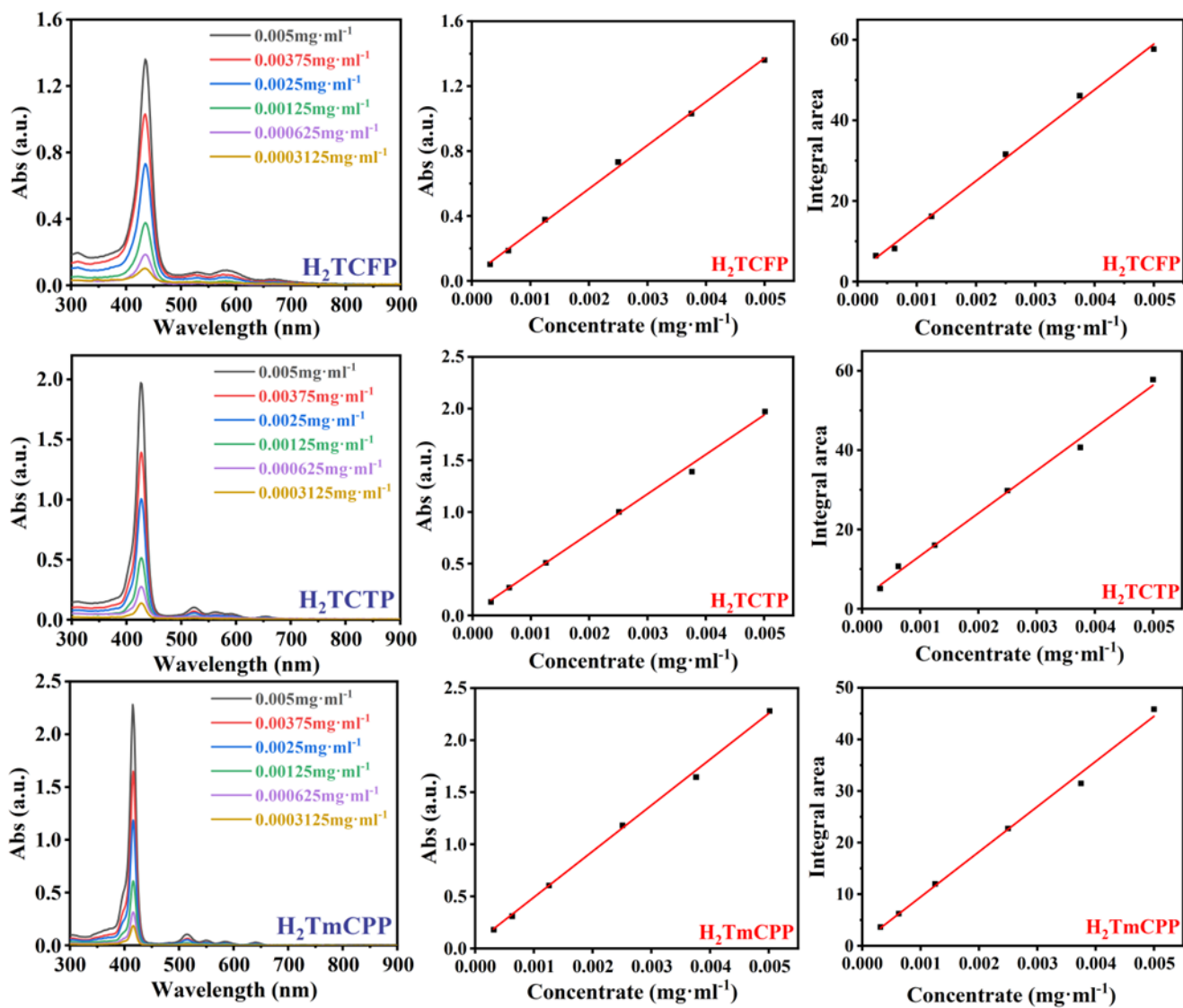**ESI**

Improving Photocatalytic Activity of Porphyrin on Hydrogen Evolution from Water Splitting through Combined Effects Inspired by meso-Carboxyfuryl Substitution

Zhou Zhou, Guo-Lei Zhang, Yue-Xin Song   and Ying-Hui Zhang *

School of Materials Science and Engineering, No.38 Tongyan Road, Jinnan District, Tianjin , P.R. China 300350,
Email: zhangyhi@nankai.edu.cn.

Figure S1. Spectra of three types of porphyrins at different concentration (left column), the standard curve (middle column) of absorbance (B band) vs. concentrations, and the standard curve (right column) of integral absorbance (350~500 nm) vs. concentrations. The linear relationship reveals that Lamber-Beer law is validated under the testing conditions.

Table S1. The wavelength of UV-vis absorption bands (in nm) for porphyrins of 0.005 mg·mL^{-1}

Porphyrin	Soret Band (nm)	ε [b] (10^2 mg^{-1}·mL·cm^{-1})	ε [c] (10^4 mg^{-1}·mL·cm^{-1})	Q Band (nm)
H$_2$TCFP	435 (30 [a])	2.68	1.13	529, 581[d], 666
H$_2$TCTP	427 (19 [a])	3.80	1.07	523, 564, 592, 653
H$_2$TmCPP	416 (12 [a])	4.39	0.87	514, 550, 586, 640

[a]：full width at half maximum for porphyrin sample of 0.005 mg·mL^{-1}; [b]: the ε of B band; [c]: the integral ε over the range of 350~500 nm; [d]: overlapped by two bands

Table S2. Some selected electron transition data of H$_2$TCFP predicted by TD-DFT calculation together with the orbital
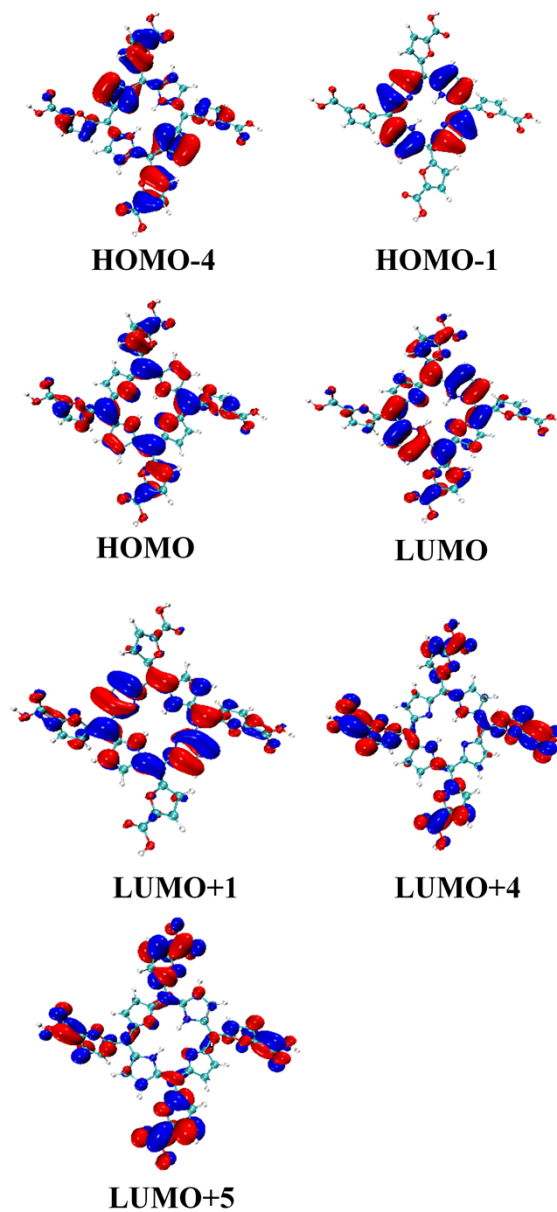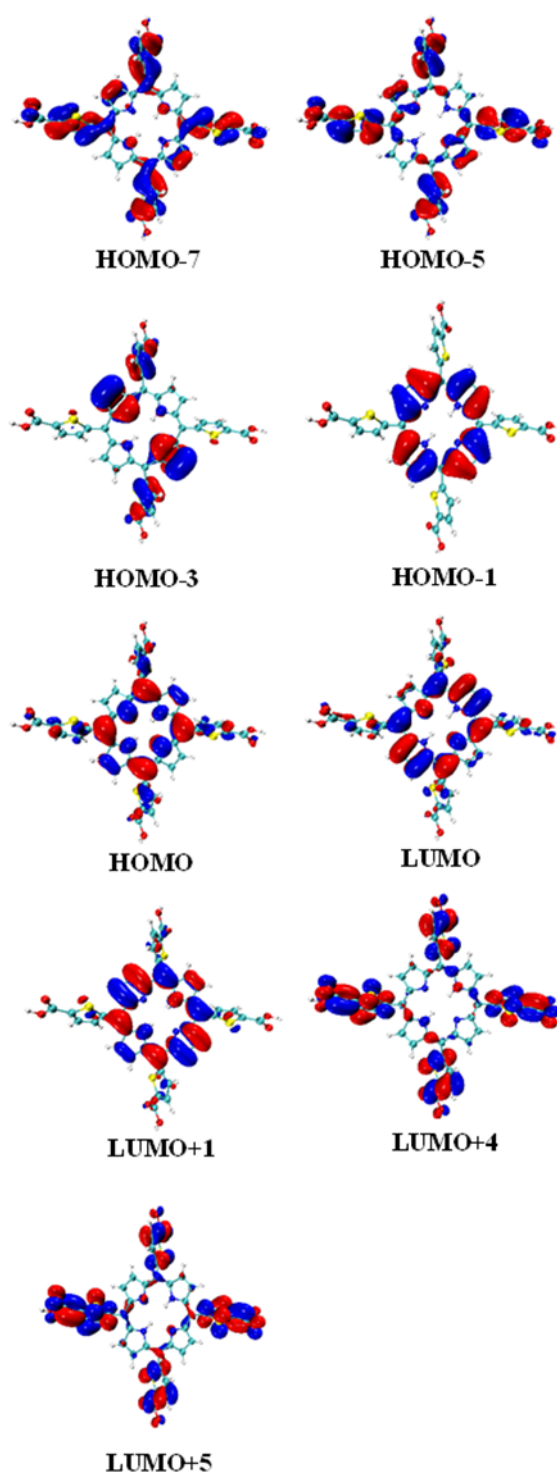

HOMO-4　　　　**HOMO-1**

HOMO　　　　**LUMO**

LUMO+1　　　　**LUMO+4**

LUMO+5

pictures.

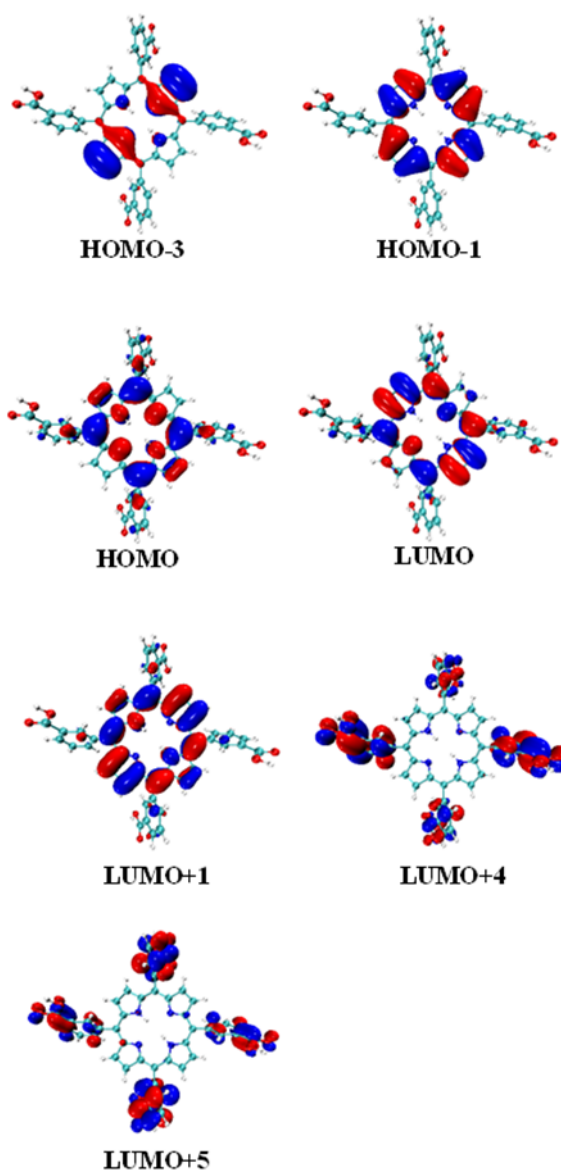| Exciting state	Transition structure	Contribution of transition (%)	Wavelength (nm) [a]	Oscillator (f) intensity
S1(Q)	HOMO-1→LUMO	27.86	659.83	0.0802
	HOMO-1→LUMO+1	2.95		
	HOMO→LUMO	9.46		
	HOMO→LUMO+1	58.92		
S2(Q)	HOMO-1→LUMO	3.69	627.05	0.2154
	HOMO→LUMO+1	20.38		
	HOMO→LUMO	66.89		
	HOMO→LUMO+1	8.80		
S3(B)	HOMO-7→LUMO+1	2.14	451.95	1.2506
	HOMO-4→LUMO+1	3.36		
	HOMO-1→LUMO	61.20		
	HOMO→LUMO+1	28.06		
S4(B)	HOMO-7→LUMO	3.05	438.55	1.1884
	HOMO-1→LUMO+1	70.47		
	HOMO→LUMO	22.37		
	HOMO→LUMO+5	2.94		
S7	HOMO-5→LUMO	14.72	406.54	0.2504
	HOMO-5→LUMO+1	11.58		
	HOMO-4→LUMO	48.96		
	HOMO-4→LUMO+1	19.65		
S10	HOMO-5→LUMO	3.84	399.52	0.0474
	HOMO-5→LUMO+1	15.46		
	HOMO-4→LUMO	30.78		
	HOMO-4→LUMO+1	45.27		
S12	HOMO-5→LUMO	74.40	387.20	0.0350
	HOMO-4→LUMO	16.80		
	HOMO→LUMO+4	5.28		
S14	HOMO-5→LUMO+1	67.87	379.44	0.2188
	HOMO-4→LUMO+1	27.13		
S17	HOMO-7→LUMO+1	4.44	354.97	0.0543
	HOMO-5→LUMO	3.57		
	HOMO→LUMO+4	85.39		
S19	HOMO-7→LUMO	11.39	349.51	0.0332
	HOMO→LUMO+5	83.94		

[a]: the transition energy is scaled by a factor of 0.9614.

Table S3. Some selected electron transition data of H_2TCTP predicted by TD-DFT calculation together with the orbital

Exciting state	Transition structure	Contribution of transition (%)	Wavelength (nm) [a]	Oscillator (f) intensity
S1(Q)	HOMO-1→LUMO	36.66	614.11	0.0241
	HOMO→LUMO+1	62.25		
S2(Q)	HOMO-1→LUMO+1	33.80	578.89	0.0804
	HOMO→LUMO	65.60		
S3(B)	HOMO-7→LUMO+1	3.27	430.03	1.0353
	HOMO-3→LUMO+1	10.87		
	HOMO-1→LUMO	50.45		
	HOMO→LUMO+1	27.44		
	HOMO→LUMO+4	4.91		
S4(B)	HOMO-7→LUMO	3.51	418.71	1.2650
	HOMO-1→LUMO+1	53.96		
	HOMO→LUMO	28.68		
	HOMO→LUMO+5	11.85		
S8	HOMO-5→LUMO+1	2.34	387.92	0.2457
	HOMO-3→LUMO+1	56.36		
	HOMO→LUMO+1	2.10		
	HOMO→LUMO+4	36.36		
S10	HOMO-3→LUMO	91.76	385.23	0.1094
	HOMO-3→LUMO+1	2.28		
S11	HOMO-7→LUMO+1	2.52	380.77	0.1841
	HOMO-5→LUMO	21.38		
	HOMO-3→LUMO+1	19.23		
	HOMO-1→LUMO	3.62		
	HOMO→LUMO+1	2.56		
	HOMO→LUMO+4	42.24		
S12	HOMO-7→LUMO	5.29	376.99	0.0418
	HOMO-5→LUMO+1	4.61		
	HOMO-3→LUMO	3.89		
	HOMO-1→LUMO+1	3.21		
	HOMO-1→LUMO+4	3.15		
	HOMO→LUMO+5	73.46		
S17	HOMO-5→LUMO	3.02	366.03	0.0305
	HOMO-5→LUMO+1	85.59		
	HOMO-1→LUMO+4	2.28		
	HOMO→LUMO+5	3.98		

[a]: the transition energy is scaled by a factor of 0.9614.

HOMO-7

HOMO-5

HOMO-3

HOMO-1

HOMO

LUMO

LUMO+1

LUMO+4

LUMO+5

pictures.

Table S4. Some selected electron transition data of H_2TmCPP predicted by TD-DFT calculation together with the orbital pictures.

Exciting state	Transition structure	Contribution of transition (%)	Wavelength (nm) [a]	Oscillator (f) Intensity
S1(Q)	HOMO-1→LUMO	34.26	601.58	0.0212
	HOMO→LUMO+1	64.70		
S2(Q)	HOMO-1→LUMO+1	35.97	562.97	0.0415
	HOMO→LUMO	63.34		
S3(B)	HOMO-3→LUMO+1	19.04	413.16	0.8338
	HOMO-1→LUMO	50.39		
	HOMO→LUMO+1	23.86		
	HOMO→LUMO+5	4.58		
S4(B)	HOMO-3→LUMO	3.84	401.99	1.0652
	HOMO-1→LUMO+1	47.71		
	HOMO→LUMO	28.00		
	HOMO→LUMO+4	16.95		
S9	HOMO-3→LUMO	2.91	379.72	0.2851
	HOMO-1→LUMO+1	9.31		
	HOMO→LUMO	5.55		
	HOMO→LUMO+4	75.31		
	HOMO→LUMO+5	4.46		
S11	HOMO-3→LUMO	90.76	364.28	0.2311
	HOMO-1→LUMO+1	3.87		
	HOMO-1→LUMO+5	2.13		
S12	HOMO-3→LUMO+1	60.49	363.19	0.7222
	HOMO-1→LUMO	10.47		
	HOMO-1→LUMO+4	11.55		
	HOMO→LUMO+1	8.29		
	HOMO→LUMO+5	7.24		
S15	HOMO-3→LUMO+1	3.40	350.74	0.1026
	HOMO-1→LUMO+4	64.3		
	HOMO-1→LUMO+5	24.73		
S16	HOMO-1→LUMO+4	22.21	350.19	0.1045
	HOMO-1→LUMO+5	69.21		

[a]: the transition energy is scaled by a factor of 0.9614.

HOMO-3

HOMO-1

HOMO

LUMO

LUMO+1

LUMO+4

LUMO+5
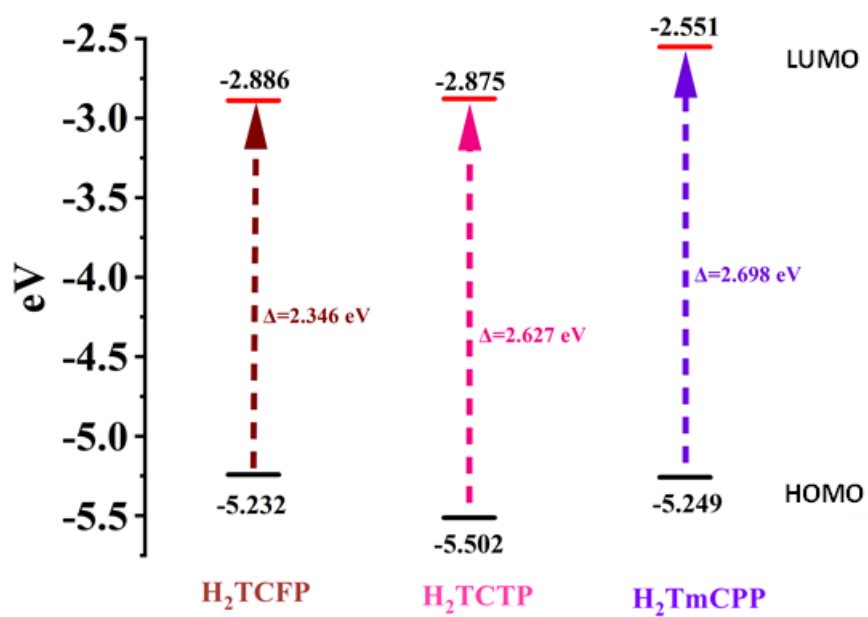
Figure S2. Predicted energy level of HOMO and LUMO orbits of three porphyrins based on TD-DFT calculations.
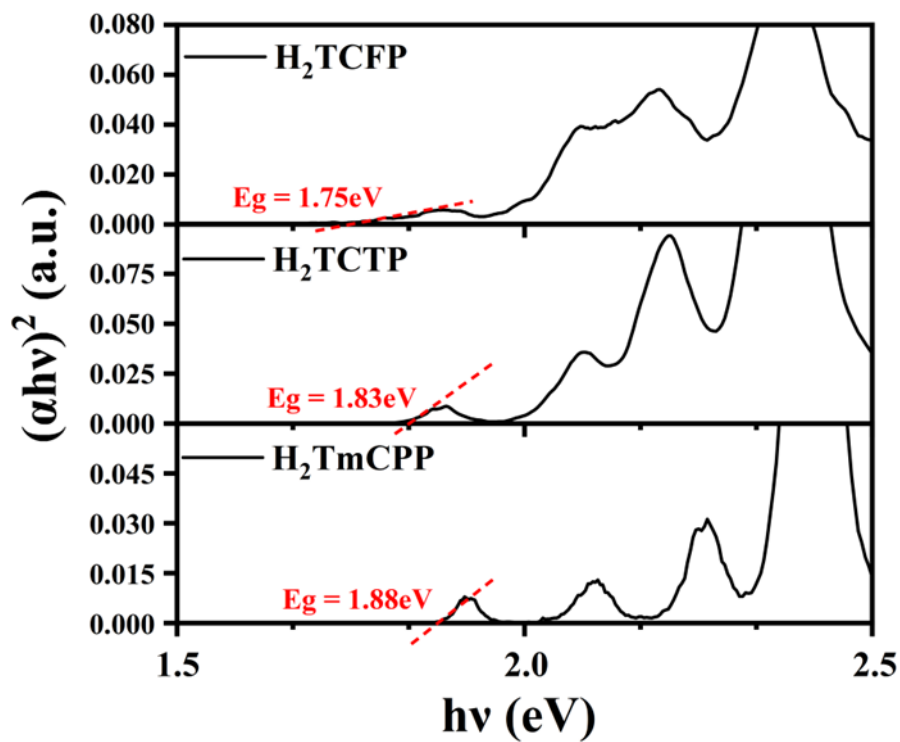
Figure S3. Tauc plot of three porphyrins derived from liquid state absorption spectra shown in Figure 1 of the text.
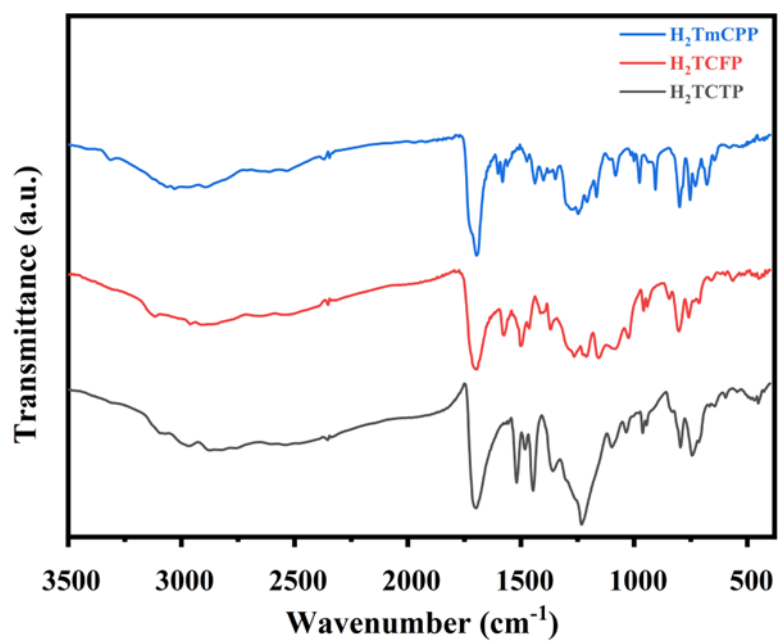
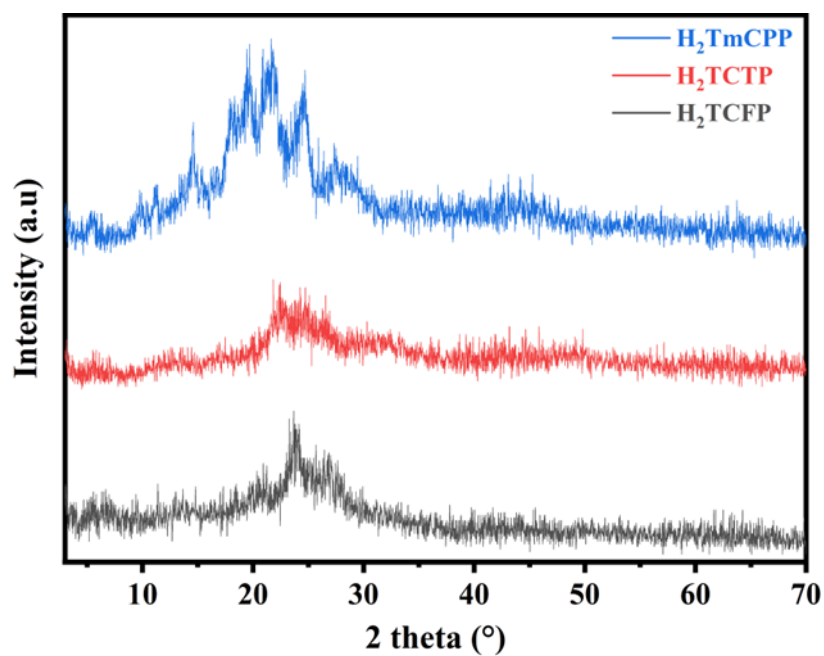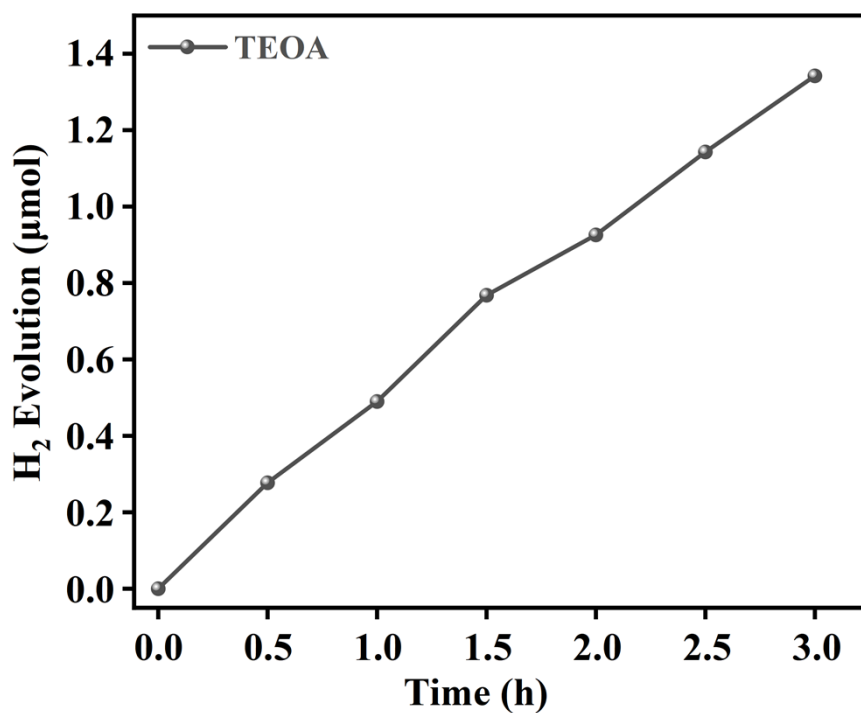**Figure S4.** FTIR spectra of H_2TmCPP, H_2TCFP and H_2TCTP.

Figure S5. XRD spectra of H_2TmCPP, H_2TCTP and H_2TCFP.

Figure S6. H_2 production profile of TEOA solution (10%)

Table S5. Comparison of the hydrogen production performance of H_2TCFP and H_2TCTP with porphyrin molecules or their compounds reported in recent years.

Sample Name	Hydrogen Evolution Rate ($\mu mol \cdot g^{-1} \cdot h^{-1}$)	Ref
H_2TCFP	10800	This Work
H_2TCTP	9700	This Work
TCPP/Pt/g-C_3N_4	1208	J Colloid Interface Sci 2017, 506, 58-65
SA-TCPP	40.8	Adv. Mater. 2019, 31, 1806626
SA-TPyP	0.8	Adv. Mater. 2019, 31, 1806626
2% NP/g-C_3N_4	2297	Appl. Surf. Sci. 499 (2020) 143755
g-C_3N_4-Cu-TCPP	~1683	Appl. Catal. B 268 (2020) 118434
5% Cu_2O/THPP	~157.5	Appl. Catal., B 211 (2017) 296–304
30% ZnTHPP/CdS NSs	68.9	Adv. Funct. Mater.2019, 29, 1902992
GO-Co-DPyP	546.5	Nanoscale,2018,10,18635–18641
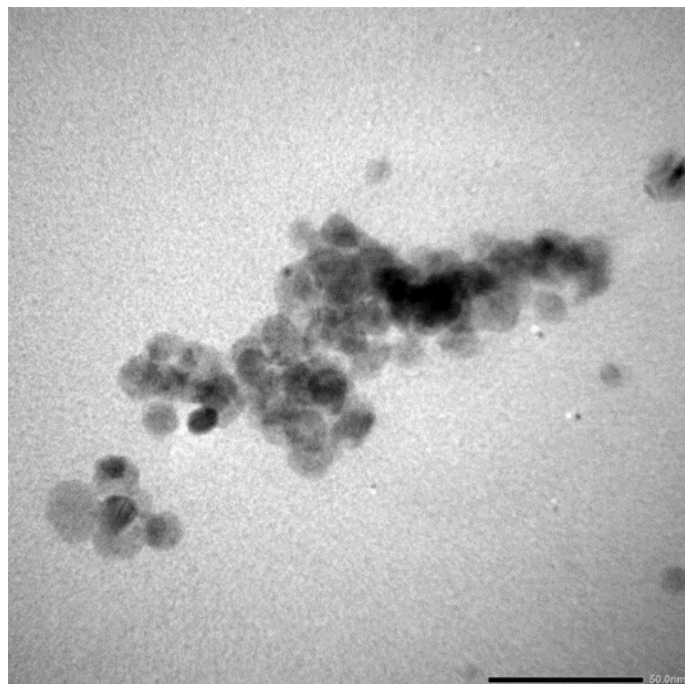
Figure S7. TEM image of H$_2$TCFP of 0.2 mg·mL^{-1} in 10% TEOA aqueous solution. Small particles of ~10 nm appear and agglomerate intensively into much larger particle.
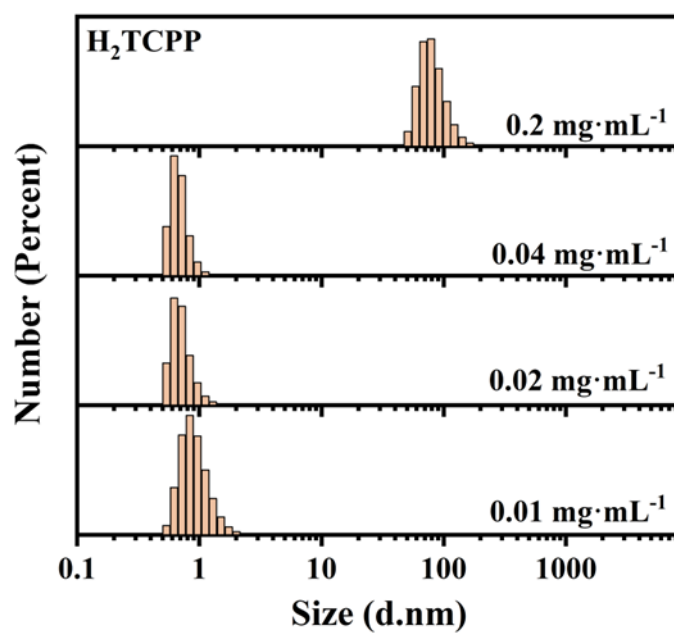
Figure S8. Variation of the DLS spectra of H$_2$TCPP with concentration.

a

2.009 Å

1.757 Å

E_{aaso}=13.13 kcal/mol

b

2.180 Å

E_{aaso}= 7.99 kcal/mol
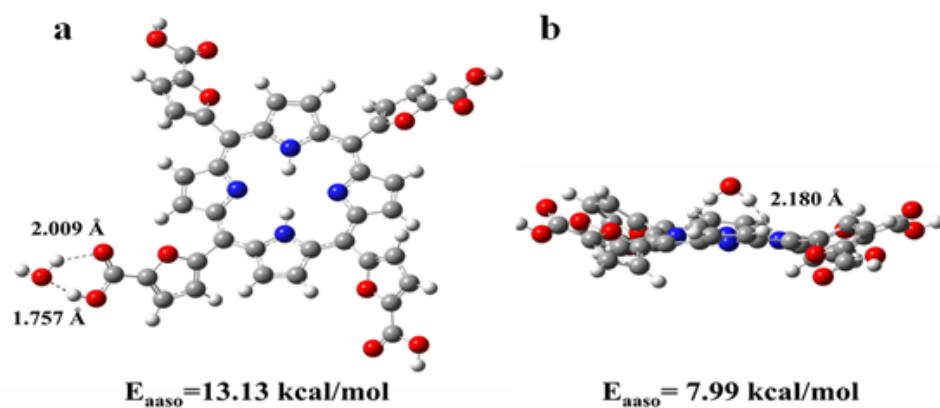
Figure S9. Two predicted association modes of H_2O molecule with H_2TCFP and the association energy $E_{asso.}$ (E_{asso}= E(porphyrin/H_2O)-E(porphyrin)-E(H_2O)-E_{bsse})

S1   S2   S3

S4   S17   S19
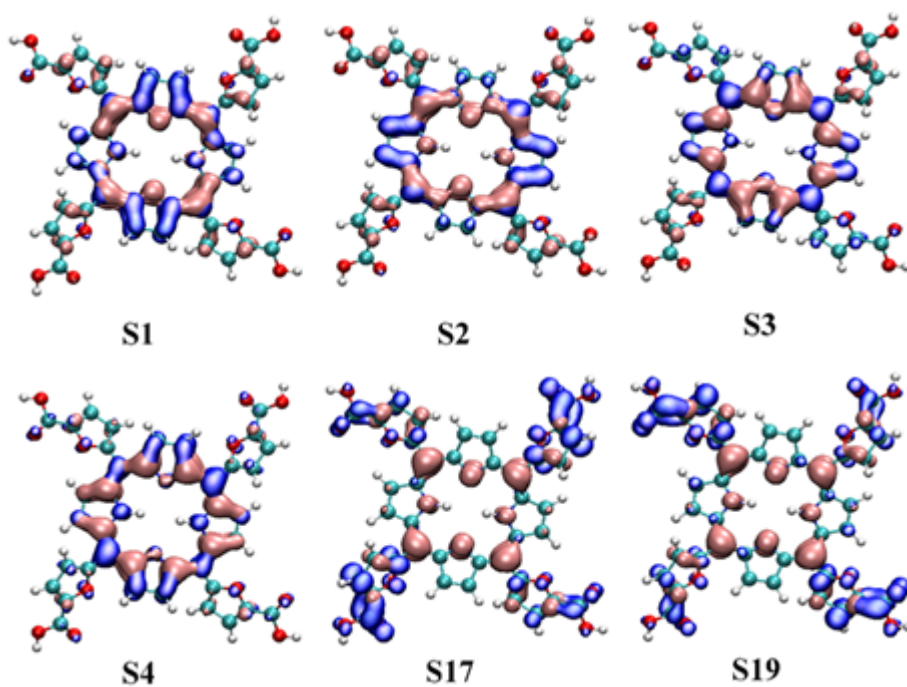
Figure S10. Photogenerated carrier distribution of certain electron excitation states for H_2TCFP predicted by TD-DFT calculation (pink: photogenerated hole distribution, blue: photogenerated electron distribution).
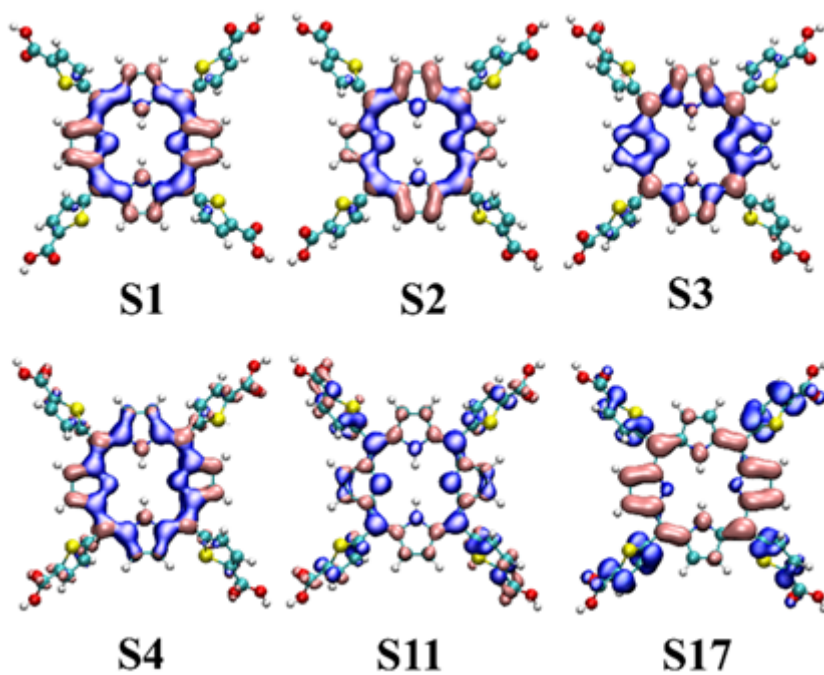
Figure S11. Photogenerated carrier distribution of certain electron excitation states for H₂TCTP predicted by TD-DFT calculation (pink: photogenerated hole distribution, blue: photogenerated electron distribution).
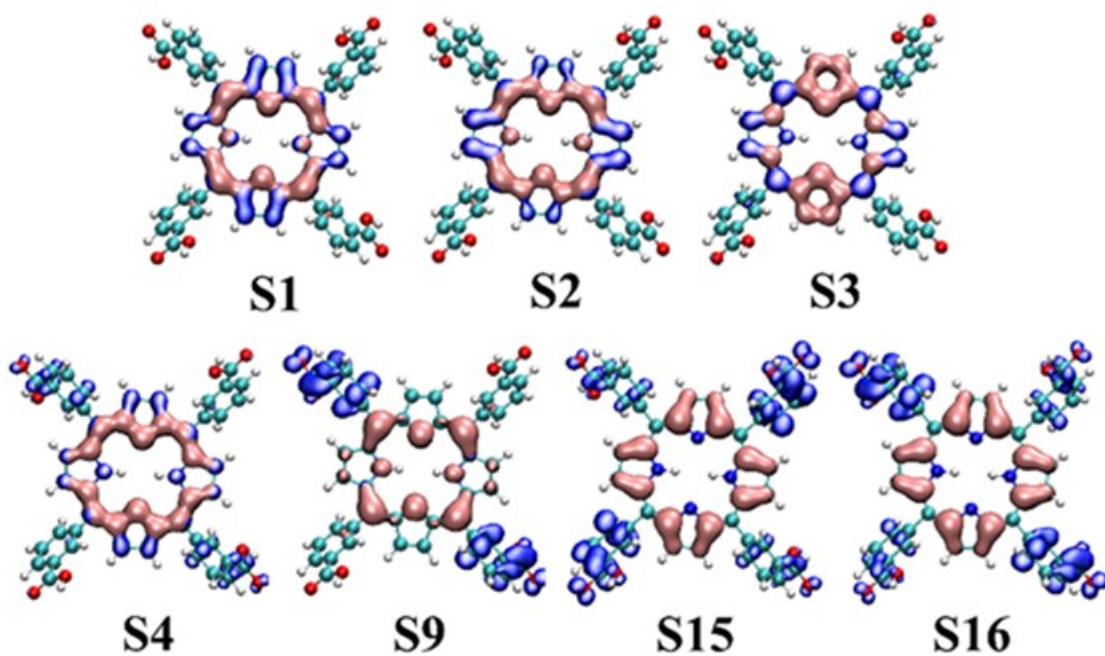
Figure S12. Photogenerated carrier distribution of certain electron excitation states for H₂TmCPP predicted by TD-DFT calculation (pink: photogenerated hole distribution, blue: photogenerated electron distribution).
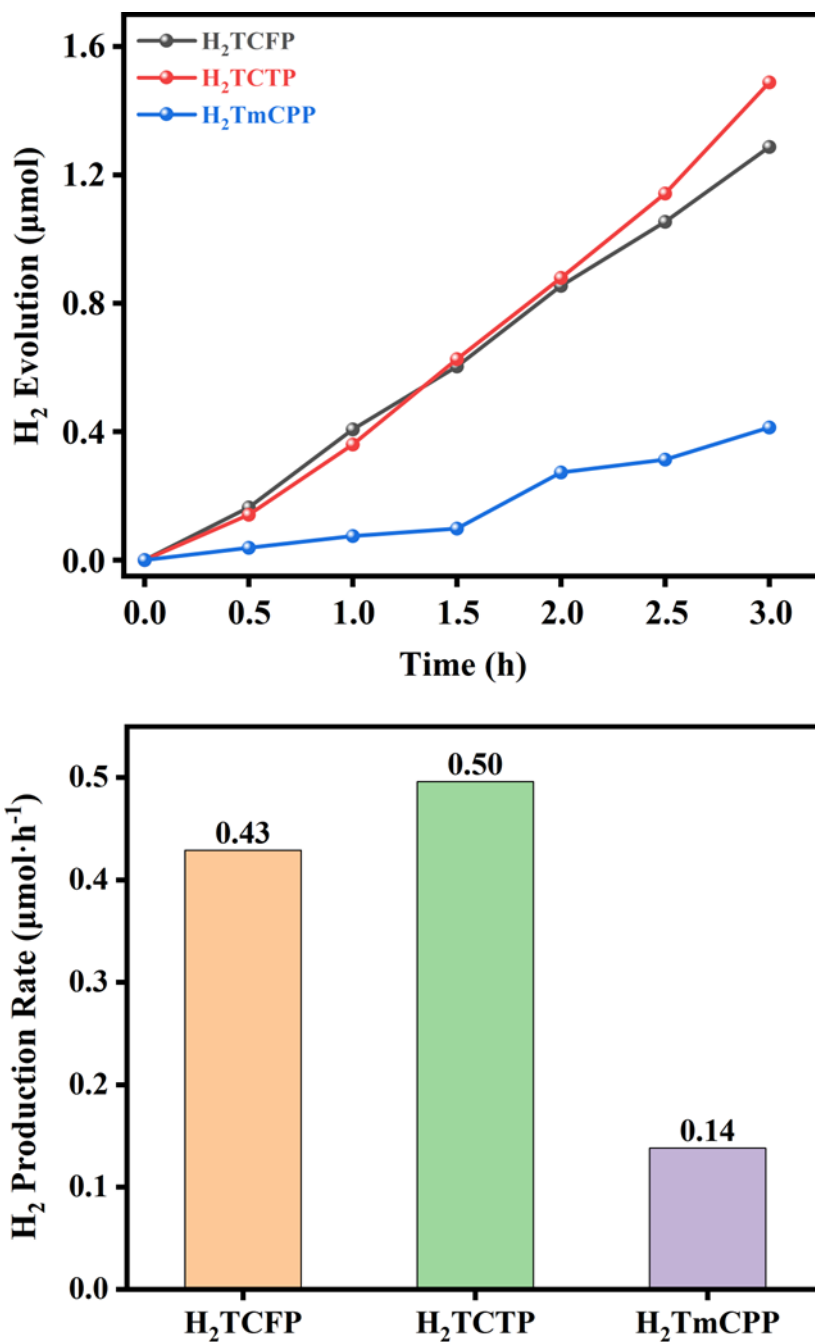
Figure S13. Hydrogen evolution profile (up) and production rates (bottom) photocatalyzed by H_2TCFP, H_2TCTP, and H_2TmCPP at 0.02 mg·mL^{-1} under UV light. ($\lambda < 365$ nm).
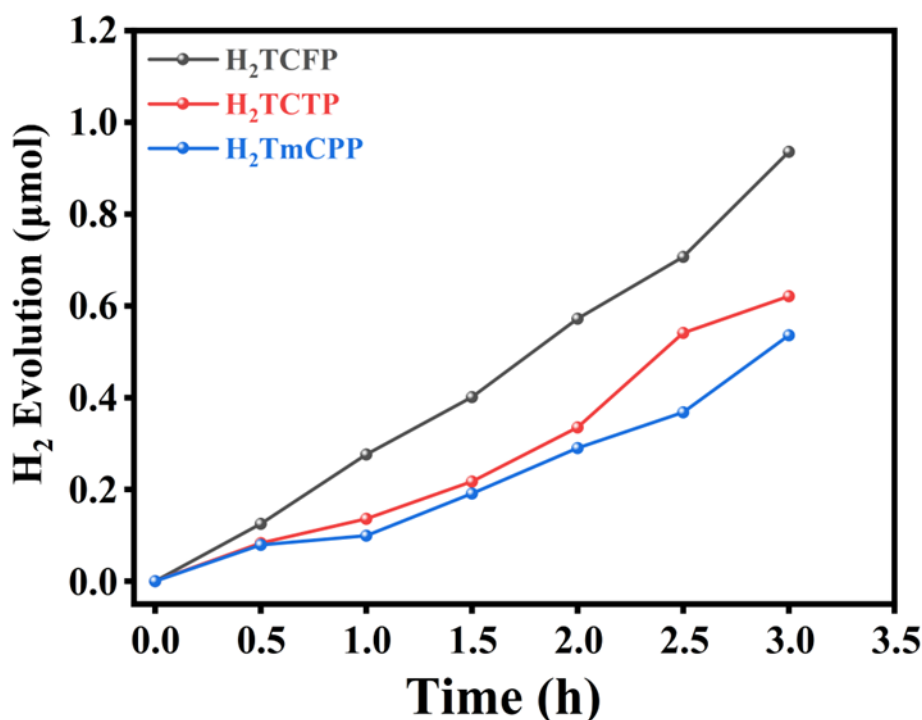
Figure S14. Hydrogen evolution profile photocatalyzed by H_2TCFP, H_2TCTP, and H_2TmCPP at 0.04 mg·mL^{-1} under UV light. ($\lambda = 365$ nm).

Calculation of Apparent Quantum Yield (AQY):

To assess the incident photon flux, we measured the intensity of monochromatic light at 365nm using a standard photovoltaic cell calibrated to AIST in a solar cell i-v tester (SAN-E1, XES-70S1), while the recorded intensities were 14.3 mW·cm^{-2}. The calculated number of incident photons (N) over a 3-hour period is 2.84×10^{20}, as determined by the equation:

$$N(365\ nm) = \frac{E\lambda}{hc} = \frac{14.3 \times 10^{-3} \times 3 \times 3600 \times 365 \times 10^{-9}}{6.626 \times 10^{-34} \times 3 \times 10^{8}} = 2.84 \times 10^{20}$$

The equation used to determine the apparent quantum yield for H_2 production (AQY-H_2) is as follows:

$$AQY = \frac{Number\ of\ evolved\ H_2\ molecules \times 2}{Number\ of\ incident\ photons} \times 100\%$$

$$AQY(H_2TCFP) = \frac{number(H_2)}{number(incident\ photons)} = \frac{0.936 * 10^{-6} * 6.02 * 10^{23} * 2}{0.284 * 10^{21}} = 0.4\%$$

$$AQY(H_2TCTP) = \frac{number(H_2)}{number(incident\ photons)} = \frac{0.621 * 10^{-6} * 6.02 * 10^{23} * 2}{0.284 * 10^{21}} = 0.26\%$$

$$AQY(H_2TmCPP) = \frac{number(H_2)}{number(incident\ photons)} = \frac{0.536 * 10^{-6} * 6.02 * 10^{23} * 2}{0.284 * 10^{21}} = 0.23\%$$
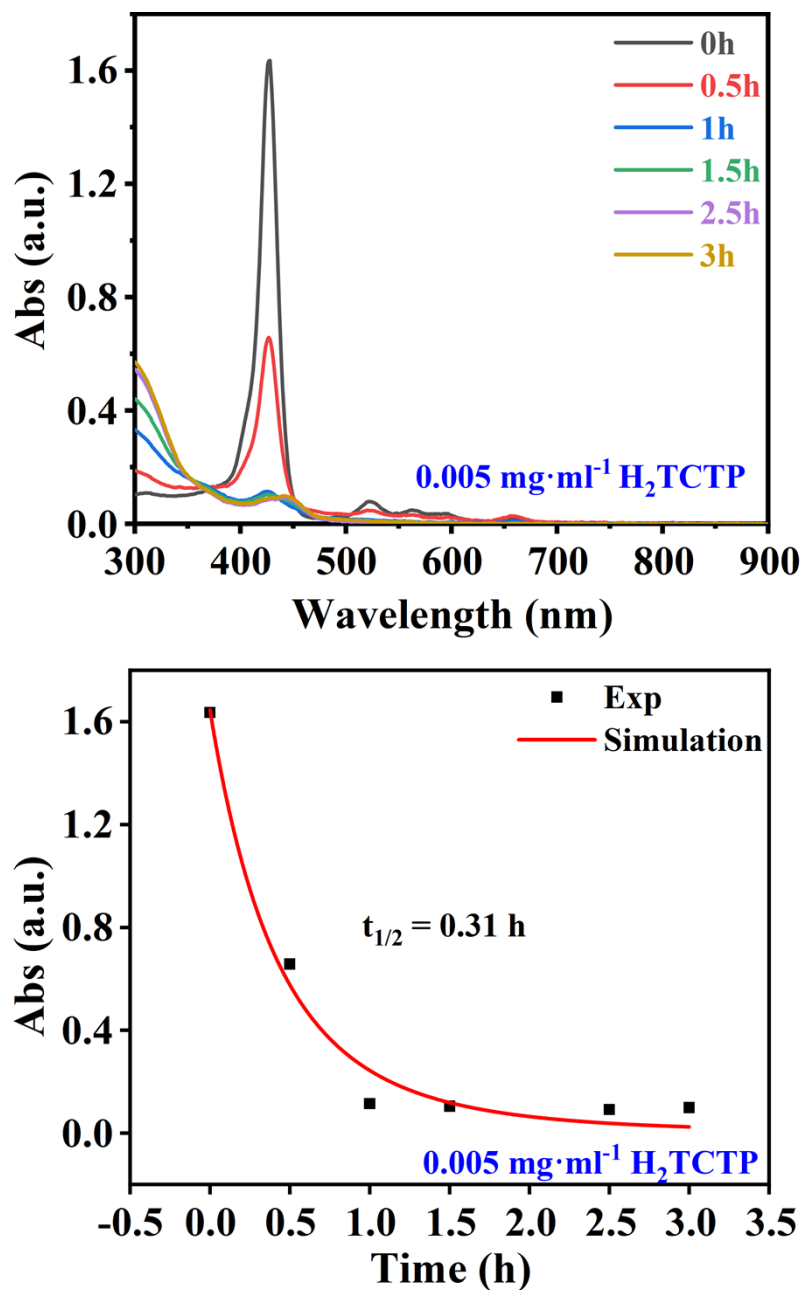
Figure S15. Variation of UV-vis spectra with irradiation time for 0.005 mg·mL^{-1} of H$_2$TCTP (upper) and the dynamics simulation (bottom). The linear relation between absorbance and time reveals a pseudo first order reaction under the situation with a t$_{1/2}$= 0.31 h.
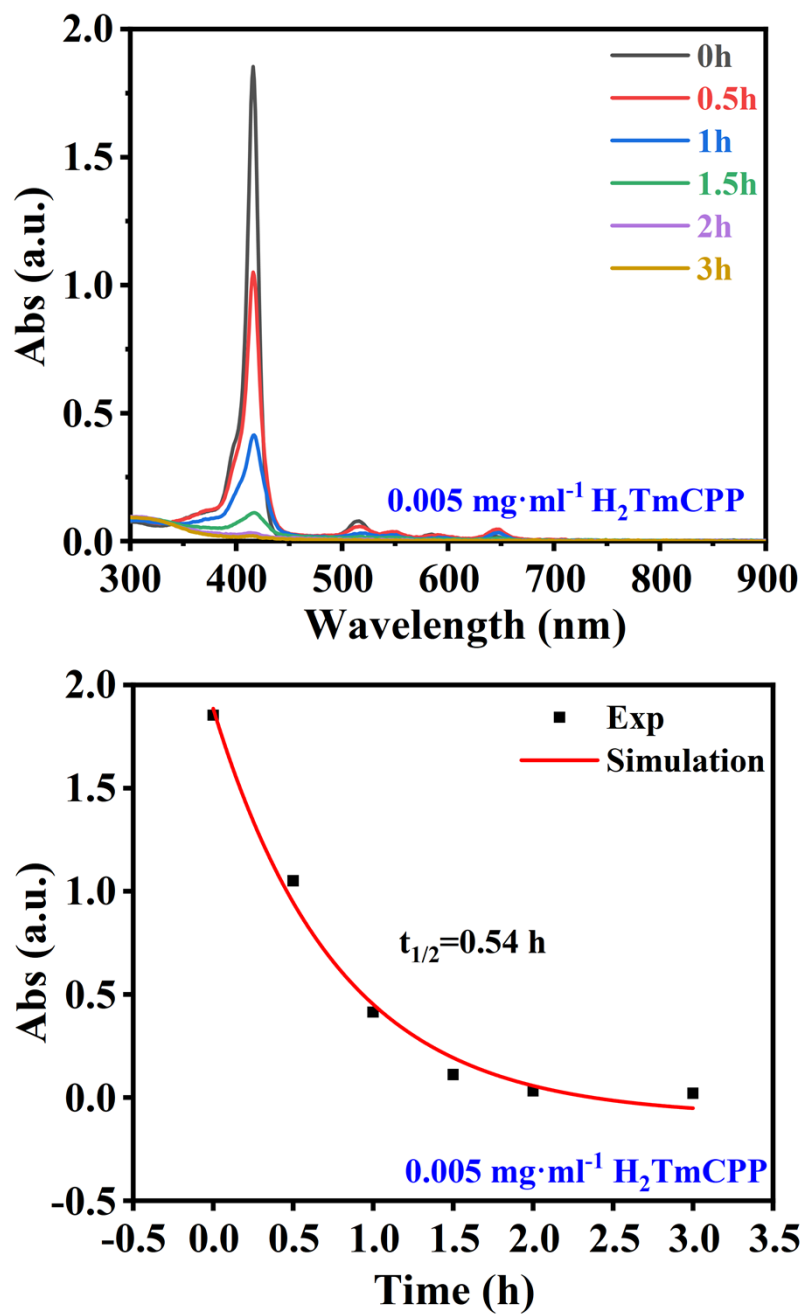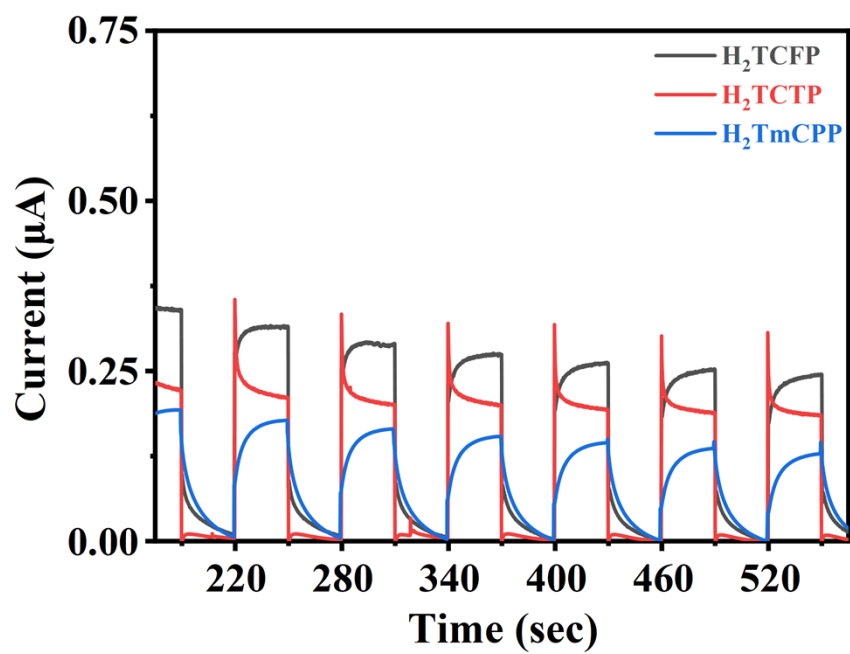
Figure S16. Variation of UV-vis spectra with irradiation time for 0.005 mg·mL^{-1} of H$_2$TmCPP (upper) and the dynamics simulation (bottom). The linear relation between absorbance and time reveals a pseudo first order reaction under the situation with a t$_{1/2}$= 0.54 h.

Figure S17. Transient photocurrents of H_2TCFP, H_2TCTP and H_2TmCPP.
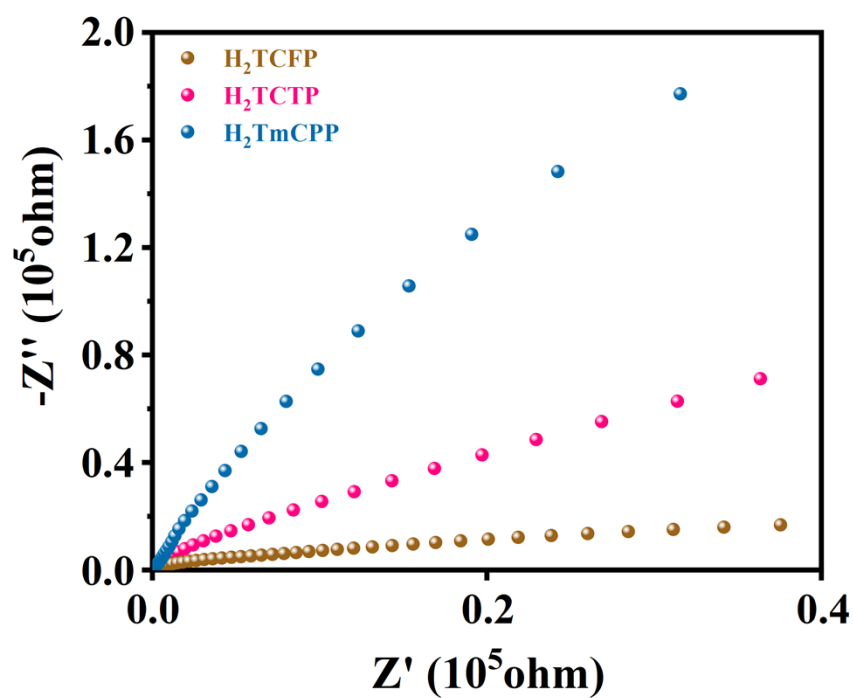
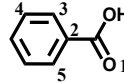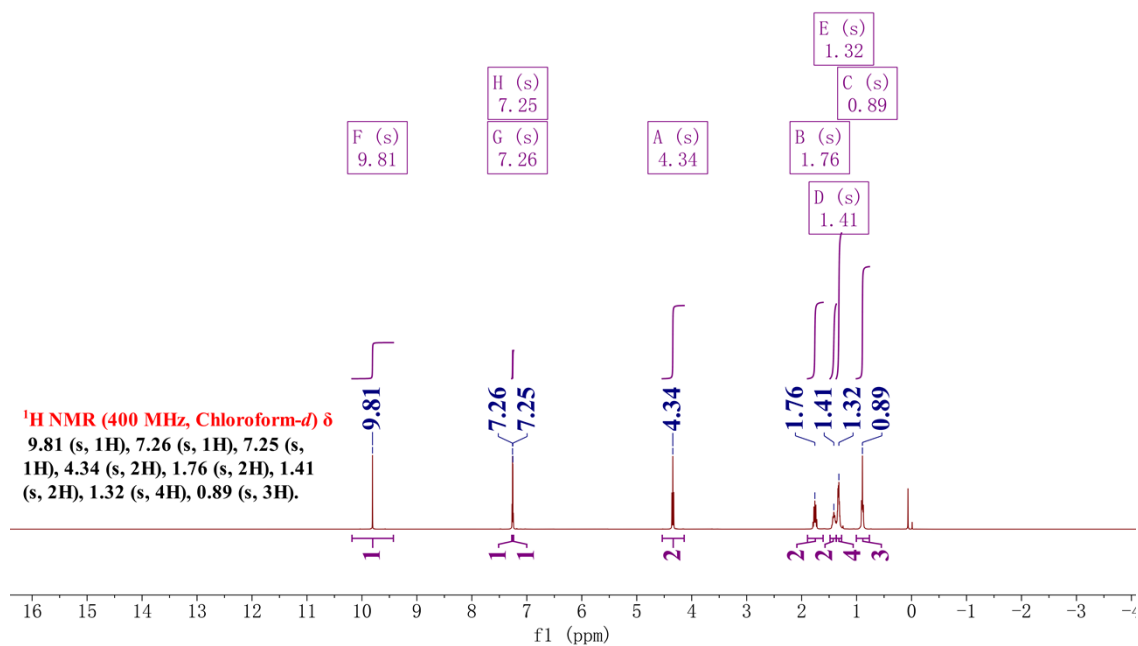**Figure S18.** Electrochemical impedance spectroscopies of H_2TCFP, H_2TCTP and H_2TmCPP.
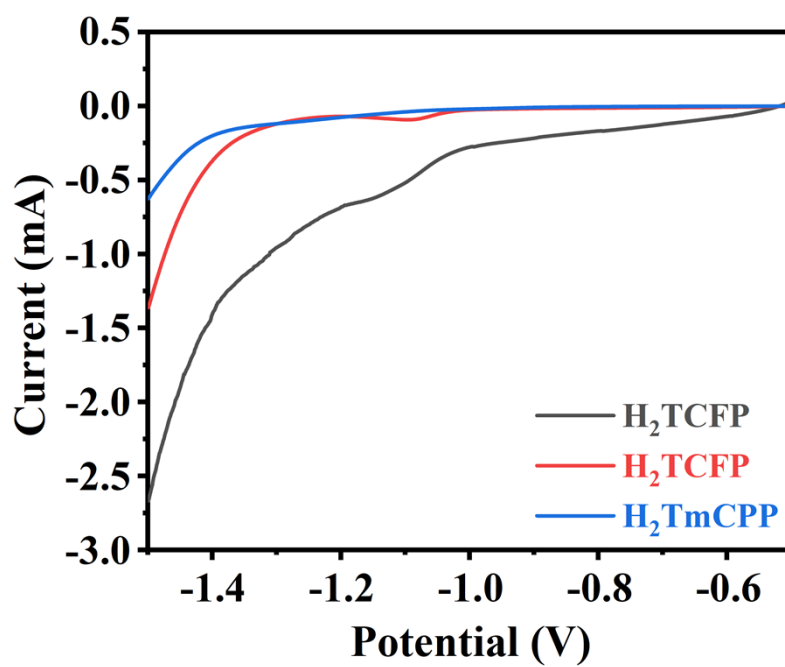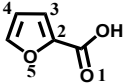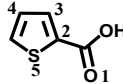
**Figure S19.** Linear sweep voltammetry test of H_2TCFP, H_2TCTP and H_2TmCPP.
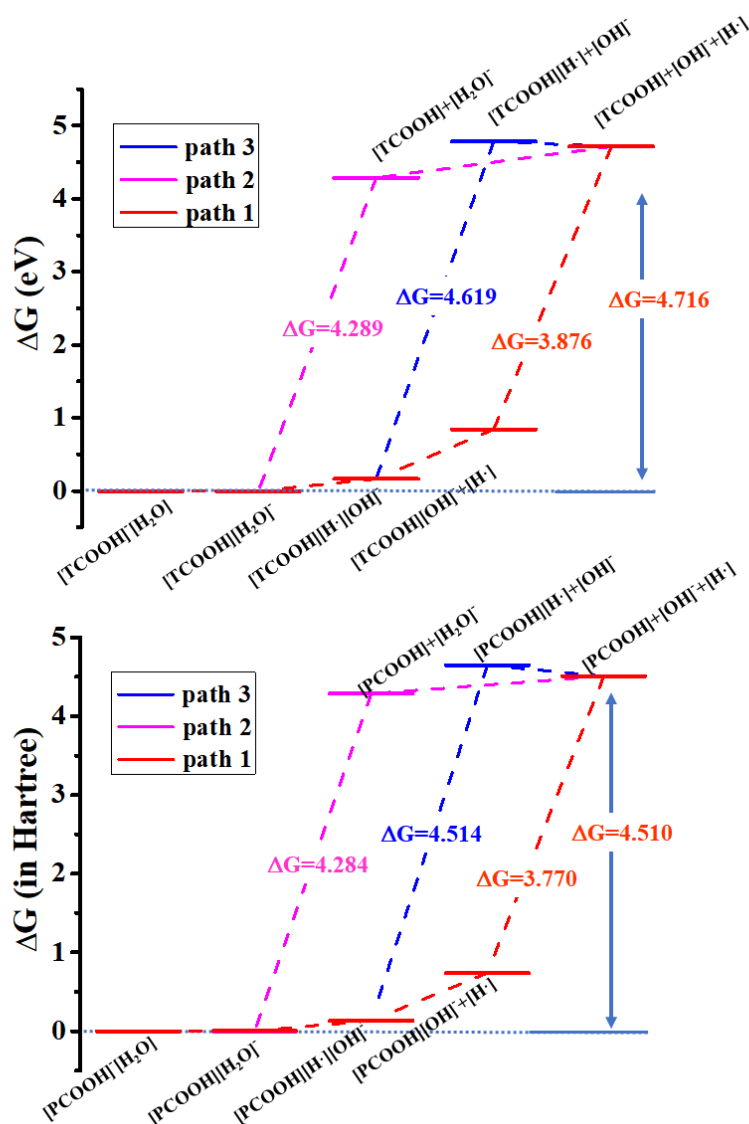
Figure S20. Dynamic processes and the change of Gibbs energy (ΔG in eV) for the splitting of water molecule associated with thiophenic acid anion (upper), and benzoic acid anion (bottom).

Table S6. Gibbs energy for hydrogen binding (ΔGH, in eV) for furoic acid, thiophenic acid, and benzoic acid.

| site	Furoic acid	Thiophenic acid	Benzoic acid
1	1.855	1.812	1.695
2	1.111	1.061	1.301
3	1.074	0.991	1.140
4	1.484	1.369	1.518
5	3.320	2.496	1.665

Figure S21. ¹H NMR spectrum of hexyl 5-formylfuran-2-carboxylate (400 MHz, Chloroform-d) δ9.81 (s, 1H), 7.26 (s, 1H), 7.25 (s, 1H), 4.34 (s, 2H), 1.76 (s, 2H), 1.41 (s, 2H), 1.32 (s, 4H), 0.89 (s, 3H).
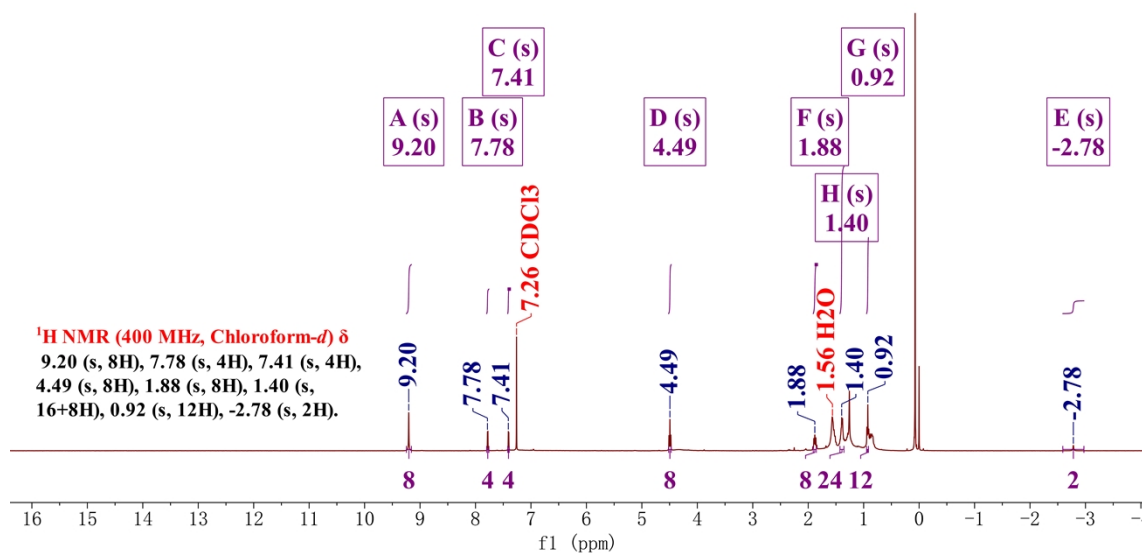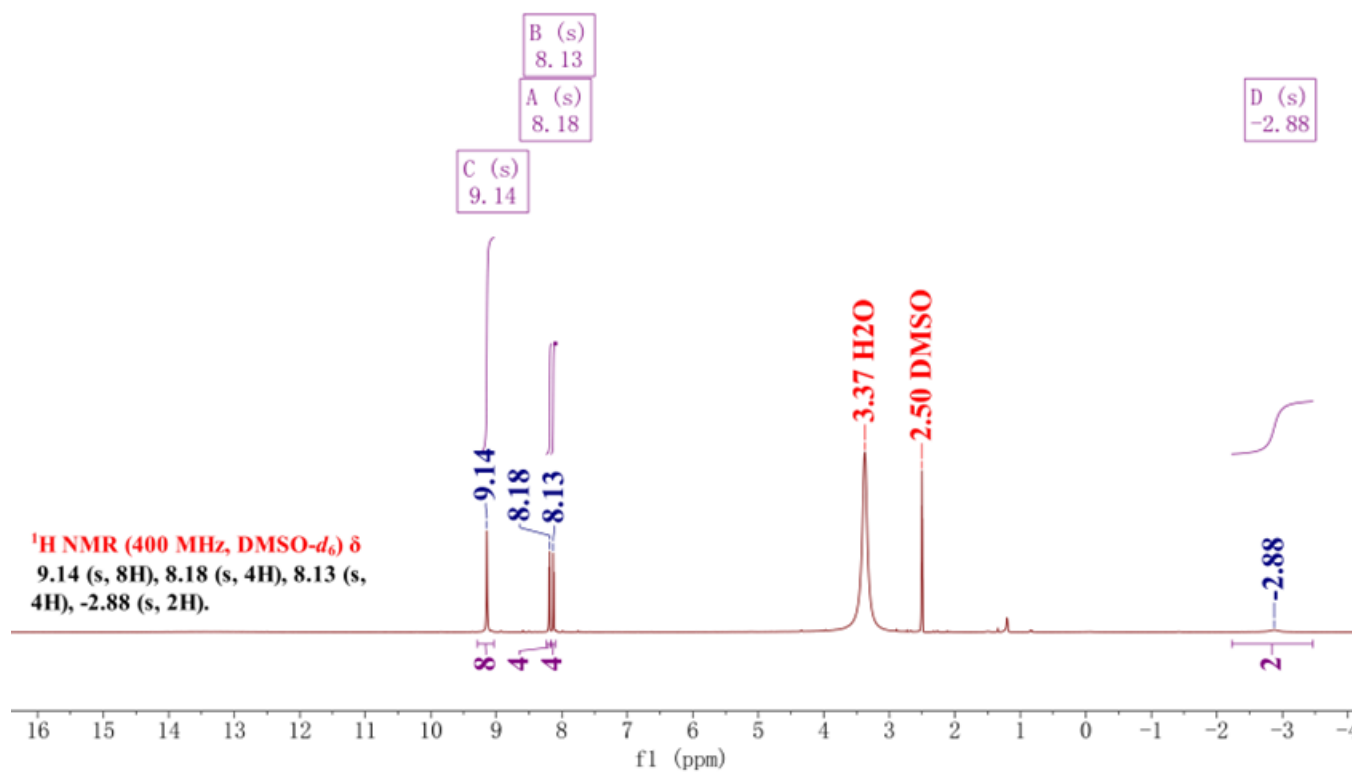

Figure S22. ¹H NMR spectrum of meso-tetra(5-hexycarboxyfuryl)porphyrin (400 MHz, Chloroform-d) δ9.20 (s, 8H), 7.78 (s, 4H), 7.41 (s, 4H), 4.49 (s, 8H), 1.88 (s, 8H), 1.40 (s, 16+8H), 0.92 (s, 12H), -2.78 (s, 2H).
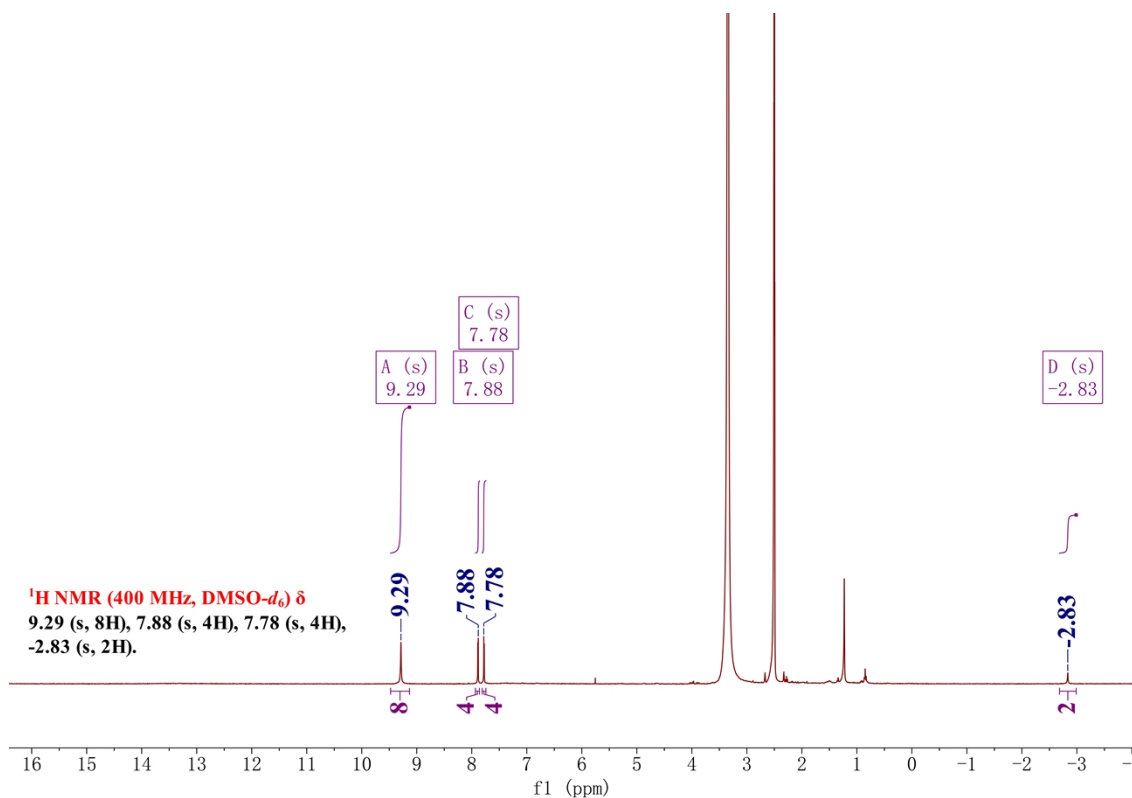
Figure S23. ¹H NMR Spectrum of meso-tetra(5-carboxyfuryl)porphyrin (400 MHz, DMSO-d6) δ 9.29 (s, 8H), 7.88 (s, 4H), 7.78 (s, 4H), -2.83 (s, 2H).
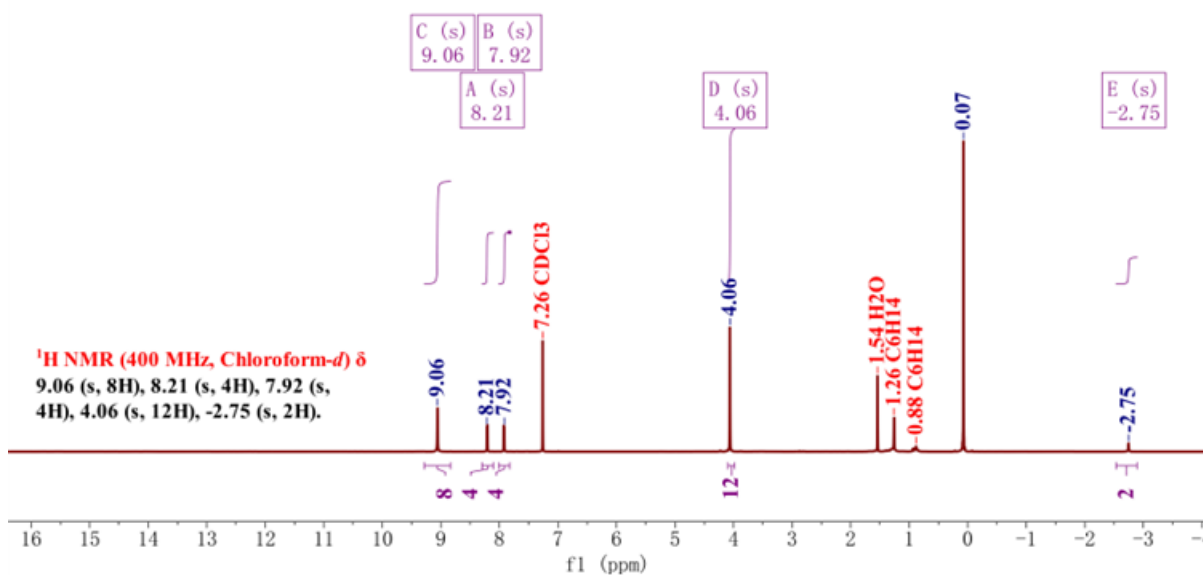
Figure S24. ¹H NMR Spectrum of meso-tetra(5-methycarboxythienyl)porphyrin (400 MHz, Chloroform-d) δ 9.06 (s, 8H), 8.21 (s, 4H), 7.92 (s, 4H), 4.06 (s, 12H), -2.75 (s, 2H).

Figure S25. ^{1}H NMR Spectrum of meso-tetra(5-carboxythienyl)porphyrin (400 MHz, DMSO-d6) δ9.14 (s, 8H), 8.1 8 (s, 4H), 8.13 (s, 4H), -2.88 (s, 2H).